

May 01, 2007

Pulsed laser ablation deposition of nanocrystalline exchange-coupled $\text{Ni}_{11}\text{Co}_{11}\text{Fe}_{67-x}\text{Zr}_7\text{B}_4\text{Cu}_x$ ($x=0,1$) films for planar inductor applications

Ashish K. Baraskar
Northeastern University

Soack Dae Yoon
Northeastern University

Anton Geiler
Northeastern University

Aria Yang
Northeastern University

C. N. Chinnasamy
Northeastern University

See next page for additional authors

Recommended Citation

Baraskar, Ashish K.; Yoon, Soack Dae; Geiler, Anton; Yang, Aria; Chinnasamy, C. N.; Chen, Yajie; Sun, Nian; Vittoria, Carmine; Goswami, Ramasis; Willard, Matthew; and Harris, Vincent G., "Pulsed laser ablation deposition of nanocrystalline exchange-coupled $\text{Ni}_{11}\text{Co}_{11}\text{Fe}_{67-x}\text{Zr}_7\text{B}_4\text{Cu}_x$ ($x=0,1$) films for planar inductor applications" (2007). *Electrical and Computer Engineering Faculty Publications*. Paper 108. <http://hdl.handle.net/2047/d20002279>

Author(s)

Ashish K. Baraskar, Soack Dae Yoon, Anton Geiler, Aria Yang, C. N. Chinnasamy, Yajie Chen, Nian Sun, Carmine Vittoria, Ramasis Goswami, Matthew Willard, and Vincent G. Harris



Pulsed laser ablation deposition of nanocrystalline exchange-coupled Ni₁₁Co₁₁Fe_{67-x}Zr₇B₄Cu_x (x = 0,1) films for planar inductor applications

Ashish K. Baraskar, Soack Dae Yoon, Anton Geiler, Aria Yang, C. N. Chinnasamy et al.

Citation: *J. Appl. Phys.* **101**, 09M519 (2007); doi: 10.1063/1.2712055

View online: <http://dx.doi.org/10.1063/1.2712055>

View Table of Contents: <http://jap.aip.org/resource/1/JAPIAU/v101/i9>

Published by the [American Institute of Physics](http://www.aip.org).

Related Articles

Structural variability in La_{0.5}Sr_{0.5}TiO_{3±δ} thin films

Appl. Phys. Lett. **99**, 261907 (2011)

Epitaxial thin films of p-type spinel ferrite grown by pulsed laser deposition

Appl. Phys. Lett. **99**, 242504 (2011)

Anomalous optical switching and thermal hysteresis behaviors of VO₂ films on glass substrate

Appl. Phys. Lett. **99**, 231909 (2011)

Increased grain boundary critical current density J_{cgb} by Pr-doping in pulsed laser-deposited Y_{1-x}Pr_xBCO thin films

J. Appl. Phys. **110**, 113905 (2011)

Temperature-dependent leakage current behavior of epitaxial Bi_{0.5}Na_{0.5}TiO₃-based thin films made by pulsed laser deposition

J. Appl. Phys. **110**, 103710 (2011)

Additional information on *J. Appl. Phys.*

Journal Homepage: <http://jap.aip.org/>

Journal Information: http://jap.aip.org/about/about_the_journal

Top downloads: http://jap.aip.org/features/most_downloaded

Information for Authors: <http://jap.aip.org/authors>

ADVERTISEMENT

LakeShore Model 8404 developed with **TOYO Corporation**
NEW AC/DC Hall Effect System Measure mobilities down to 0.001 cm²/V s

Pulsed laser ablation deposition of nanocrystalline exchange-coupled $\text{Ni}_{11}\text{Co}_{11}\text{Fe}_{67-x}\text{Zr}_7\text{B}_4\text{Cu}_x$ ($x=0, 1$) films for planar inductor applications

Ashish K. Baraskar^{a)}

Department of Electrical and Computer Engineering, Northeastern University, Boston, Massachusetts 02115

Soack Dae Yoon

Center for Microwave Magnetic Materials and Integrated Circuits, Northeastern University, Boston, Massachusetts 02115

Anton Geiler and Aria Yang

Center for Microwave Magnetic Materials and Integrated Circuits and Department of Electrical and Computer Engineering, Northeastern University, Boston, Massachusetts 02115

C. N. Chinnasamy and Yajie Chen

Center for Microwave Magnetic Materials and Integrated Circuits, Northeastern University, Boston, Massachusetts 02115

Nian Sun and Carmine Vittoria

Center for Microwave Magnetic Materials and Integrated Circuits and Department of Electrical and Computer Engineering, Northeastern University, Boston, Massachusetts 02115

Ramasis Goswami and Matthew Willard

Naval Research Laboratory, Washington, DC 20375

Vincent G. Harris

Center for Microwave Magnetic Materials and Integrated Circuits and Department of Electrical and Computer Engineering, Northeastern University, Boston, Massachusetts 02115

(Presented on 9 January 2007; received 30 October 2006; accepted 18 December 2006; published online 9 May 2007)

Nanocrystalline films of the $\text{Ni}_{11}\text{Co}_{11}\text{Fe}_{67-x}\text{Zr}_7\text{B}_4\text{Cu}_x$ ($x=0, 1$) composition were deposited on fused quartz substrates by pulsed laser deposition. For the films of $\text{Ni}_{11}\text{Co}_{11}\text{Fe}_{66}\text{Zr}_7\text{B}_4\text{Cu}$, the bcc grain size ranged from 5 to 8 nm in the films deposited at substrate temperatures from ambient to 300 °C. Films grown at a substrate temperature of 300 °C were found to have optimal magnetic properties including minima in the coercivity and ferromagnetic resonance (FMR) linewidth. The magnetic characterization studies showed coercivity $H_c < 5$ Oe, $4\pi M_S \sim 16$ kG, and in-plane uniaxial anisotropy field (H_A) ~ 25 –30 Oe. The ferromagnetic resonance linewidth was measured to be 34 Oe and zero magnetic field ferromagnetic resonance at ~ 2 GHz. These properties allow these films to be candidates for magnetic planar inductors operating from 0.5 to 2 GHz. © 2007 American Institute of Physics. [DOI: [10.1063/1.2712055](https://doi.org/10.1063/1.2712055)]

I. INTRODUCTION

With the increasing demand for smaller passive components that operate at higher frequencies and temperatures, the electronics industry is in need of improved alloys for use in thin film inductors. Specifically, these materials should possess a high permeability, high saturation magnetization, and low coercivity.^{1,2} To this end, we have prepared and studied the dc and high frequency magnetic properties of nanocrystalline exchange-coupled alloy (NECA) films. The alloys we have chosen have attractive properties when prepared as bulk ribbons¹ where they were characterized to have a nanograined microstructure in which body-centered-cubic (bcc) metallic crystallites were embedded within an amorphous matrix.² In previous work,³ the structural and magnetic properties of $(\text{Ni}_{0.67}\text{Co}_{0.25}\text{Fe}_{0.08})_{88}\text{Zr}_7\text{B}_4\text{Cu}_1$ and $(\text{Ni}_{0.67}\text{Co}_{0.25}\text{Fe}_{0.08})_{89}\text{Zr}_7\text{B}_4$ films with saturation magnetization of $4\pi M_S \sim 7000$ G were presented. In this report, we present the structure, magnetic, and microwave properties of

$\text{Ni}_{11}\text{Co}_{11}\text{Fe}_{67-x}\text{Zr}_7\text{B}_4\text{Cu}_x$ ($x=0, 1$) film alloys. The present alloy contains more iron (Fe) and resulted in films having a saturation magnetization to be near 17 kG.

Nanocrystalline soft magnetic materials (FinemetTM) were first developed by Yoshizawa *et al.* at Hitachi metals.² The addition of 1 at. % of Cu was shown by Ayers *et al.* to be of prime importance for the nucleation and growth of the nanocrystalline metallic phase.⁴ However, its role in other NECA's remains unclear. Herzer⁵ observed a power law relationship between the coercivity and the grain size ($H_c \propto D^6$) of nanostructured soft magnetic alloys and subsequently proposed a random anisotropy model that explains the soft magnetic properties. In 1998, Suzuki *et al.*⁶ demonstrated that for systems that possess a strong uniaxial anisotropy, i.e., much greater than the random magnetocrystalline anisotropy, the D^6 law did not hold but instead the correlation should be D^3 .

We found that for films having a well-defined uniaxial anisotropy, a power law relationship is observed with $H_c \propto \sim D^3$. In that earlier study, we found the best soft magnetic

^{a)}Electronic mail: baraskar.a@neu.edu

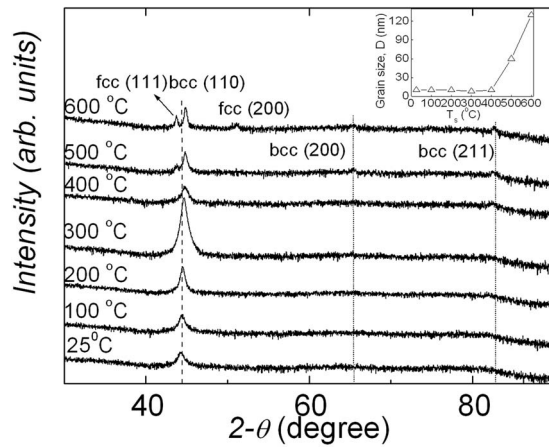


FIG. 1. X-ray diffraction of $\text{Ni}_{11}\text{Co}_{11}\text{Fe}_{66}\text{Zr}_7\text{B}_4\text{Cu}$ films deposited at the indicated temperature. The Miller indices of all diffraction peaks are indexed to bcc and fcc metallic phases. Shown in the inset is the variation of the grain size with the substrate temperature.

results were obtained from films deposited at $T_s=300^\circ\text{C}$. In this study, we present results of the optimal growth conditions for films of $\text{Ni}_{11}\text{Co}_{11}\text{Fe}_{67-x}\text{Zr}_8\text{B}_4\text{Cu}_x$ ($x=0,1$). Since this alloy has substantially higher magnetization, it offers greater potential for applications as an inductor material.

II. EXPERIMENTAL PROCEDURE

Commercially prepared 99.9% pure metal alloys of $\text{Ni}_{11}\text{Co}_{11}\text{Fe}_{67-x}\text{Zr}_7\text{B}_4\text{Cu}_x$ ($x=0,1$) were used as targets. The target contained more Fe and less Ni and Co relative to previous work³ in order to increase the magnetic moment. All the deposition conditions were similar to those described in previous work.³

Structural properties were determined by x-ray diffraction (XRD), atomic force microscopy (AFM), and transmission electron microscopy (TEM). Lattice parameters of the nanocrystalline phase were deduced using standard practices and grain size was determined by TEM and AFM.

Magnetic properties, such as coercivity, anisotropy field, remanent, and saturation magnetization (as $4\pi M_s$), were measured from hysteresis loops collected using a vibrating sample magnetometer (VSM) with the applied magnetic field aligned along both the in-plane easy and hard magnetic axes. Ferromagnetic resonance (FMR) of the films was measured using a cavity technique operating in the TE_{102} mode. Room temperature FMR spectra were taken at X-band frequency using a differential power absorption technique with a Varian microwave bridge as the microwave source and a Varian E-line console that included a built in lock-in amplifier and a 100 kHz modulation signal for detection of the absorption signal.

III. RESULTS AND DISCUSSION

A. Structure and morphology

Shown in Fig. 1 is the x-ray diffraction pattern of the $\text{Ni}_{11}\text{Co}_{11}\text{Fe}_{66}\text{Zr}_7\text{B}_4\text{Cu}$ films deposited at different substrate temperatures. As indicated in the figure, the major Bragg peaks correspond to the bcc phase.^{7,8} In films grown at

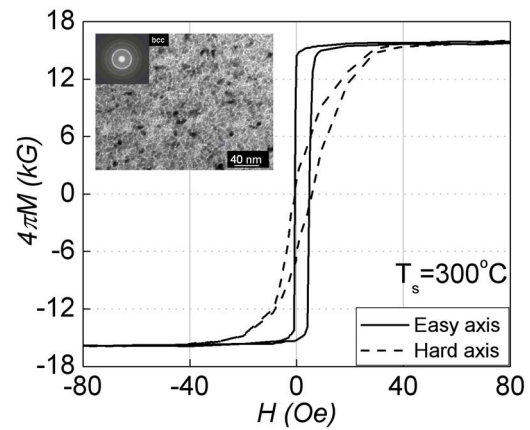


FIG. 2. Hysteresis loops for the $\text{Ni}_{11}\text{Co}_{11}\text{Fe}_{66}\text{Zr}_7\text{B}_4\text{Cu}$ film grown at 300°C . Inset shows TEM image of $\text{Ni}_{11}\text{Co}_{11}\text{Fe}_{67-x}\text{Zr}_7\text{B}_4\text{Cu}$ film grown at $T_s=300^\circ\text{C}$ showing the 5 nm crystallites surrounded by the amorphous matrix.

500°C , the bcc peaks are found to be suppressed and peaks corresponding to fcc phase⁸ are seen indicating its presence as a secondary phase. In the films grown at 600°C , more intense peaks of the fcc phase are seen which signals an increase in the fcc volume fraction with the increasing substrate temperature. The inset shows the variation of the grain size with the deposition temperature. It can be seen that the minimum grain size is obtained in the film deposited at 300°C and it is found to increase drastically in the films grown at $T_s > 400^\circ\text{C}$.

From the bcc phase peak (110), the lattice parameter was estimated to be about 0.289 nm which matches closely with the lattice parameter of Fe-rich FeCo alloys⁹ and remains constant within the uncertainty of measurements for values of $T_s \leq 300^\circ\text{C}$. It was found to decrease in the films deposited at higher temperatures which might be due the nucleation of the fcc phase and the subsequent change in bcc crystallite composition. The bcc lattice parameter at 600°C was found to be about 0.2856 nm very close to bcc iron.⁸

Figure 2 (inset) shows the high resolution transmission electron microscope (HRTEM) image for the $\text{Ni}_{11}\text{Co}_{11}\text{Fe}_{67}\text{Zr}_7\text{B}_4$ film deposited at $T_s=300^\circ\text{C}$. It can be seen that bcc grains of around 5–8 nm in diameter are surrounded by a (white) amorphous matrix that is <1 nm in thickness. The AFM results illustrate a change in topography of the films with increasing substrate temperature. The mean roughness of the films increased with increase in substrate temperature and is closely correlated to the grain size determined by TEM. Films grown at $T_s=300^\circ\text{C}$ had the lowest value of surface roughness at <2 nm (rms). Comparison of HRTEM images indicates that nanosize grains were maintained, but the size of some grains increased as T_s increased to 400°C .

B. Magnetic properties

In-plane hysteresis loops with the magnetic field aligned along the easy and hard axis were obtained for all samples. Coercivity, uniaxial anisotropy field, and remanence and saturation magnetization values were obtained from these data. Hysteresis loops for the film deposited at $T_s=300^\circ\text{C}$ are shown in Fig. 2 which indicate soft magnetic properties

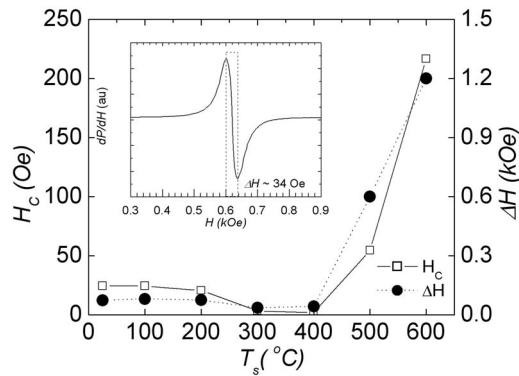


FIG. 3. Coercivity and ferromagnetic resonance derivative linewidths for $\text{Ni}_{11}\text{Co}_{11}\text{Fe}_{66}\text{Zr}_7\text{B}_4\text{Cu}$ film vs deposition temperature measured at X-band (9.6 GHz) frequency. The inset shows FMR spectrum with a minimum $\Delta H \sim 34$ Oe measured from the film grown at 300°C .

($H_c \sim 5$ Oe). The coercivity was found to increase dramatically in the samples deposited at higher temperatures which can be attributed to grain coarsening. The magnetization of the films deposited at $T_s < 400^\circ\text{C}$ had nearly a constant value of 16 kG which decreased rapidly for the samples deposited at higher temperatures which is probably due to the formation a surface oxide. Although the XRD does not show signs of this, the color of the film surface appears as a matted gray for $T_s > 400^\circ\text{C}$. Ferromagnetic resonance (FMR) measurements were performed to determine the microwave properties of the films where the FMR linewidths (ΔH) were measured at $f = 9.63$ GHz. Figure 3 is a plot of H_c and ΔH vs T_s for $x=1$ alloy. For the $\text{Ni}_{11}\text{Co}_{11}\text{Fe}_{66}\text{Zr}_7\text{B}_4\text{Cu}$ films, the lowest value of ΔH was found in films grown at $T_s = 300^\circ\text{C}$ and measured to be 34 Oe, whereas for the films of $\text{Ni}_{11}\text{Co}_{11}\text{Fe}_{67}\text{Zr}_7\text{B}_4$, the lowest value of ΔH was found to be near 100 Oe. The higher value of ΔH for the films for $\text{Ni}_{11}\text{Co}_{11}\text{Fe}_{67}\text{Zr}_7\text{B}_4$ might be due to target imperfections, i.e., irregularities or voids which in turn resulted in the appearance of voids in the films. The Lande spectroscopic splitting factor (g) for $\text{Ni}_{11}\text{Co}_{11}\text{Fe}_{66}\text{Zr}_7\text{B}_4\text{Cu}$ films was found to be 2.1. This value was deduced from the relation between resonant frequencies versus resonance field and was found to be similar to values for elemental Fe ($g=2.1$). This value is smaller than the value of 2.21 obtained by Joshi *et al.*³ which is due to the higher content of Ni and Co for which the value of g is about 2.21.

C. Coercivity, grain size, and the effect of Cu

To determine the role of Cu in the evolution of the thin film nanostructure, a comparison of the structural and magnetic properties of the films for both alloys ($x=0, 1$) deposited under the same conditions was performed. It was found that, for low temperature depositions, i.e., $T_s < 300^\circ\text{C}$, the structural and magnetic properties of the films for $x=0$ and 1 are similar. For the $x=0$ alloys, the grain size and coercivity increased rapidly with the increase in substrate temperature ($T_s > 300^\circ\text{C}$), indicating the onset of grain coarsening at lower temperatures.

Figure 4 is a plot of H_c vs D for both $x=0$ and $x=1$ alloy films. For both alloys, we observe power law dependence

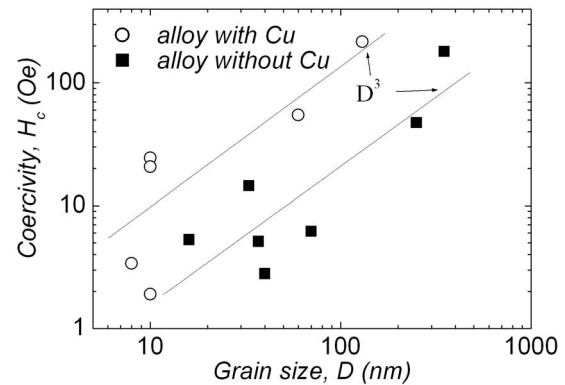


FIG. 4. Coercivity vs grain size illustrating a power law dependence for samples with and without Cu. The lines show a D^3 dependence that is expected for nanocrystalline soft magnetic thin films with an in-plane uniaxial anisotropy.

near D^3 . This is in agreement with Suzuki *et al.*,⁶ who demonstrated a deviation from D^6 to D^3 for samples that possess a long range uniaxial anisotropy (LRUA). We have found these films to possess an in-plane uniaxial anisotropy field of 25–30 Oe. However, for the two alloys the curves are shifted, indicating that the coercivity is larger for the same size crystallites for the alloy containing Cu. TEM images of this alloy illustrated voids in the microstructure. We believe that these voids arise from the PLD process and the nature of the alloy compacted target. Overall, these results are consistent with the theory postulated in Ref. 6

IV. CONCLUSIONS

The pulsed laser deposited films exist as a two phase alloy with body-centered-cubic metallic grains suspended in an amorphous matrix (with additional phases forming at elevated T_s). The softest magnetic properties (coercivity $H_c \sim 5$ Oe, $4\pi Ms \sim 16$ kG) coincided to a deposition at 300°C in which the bcc grain size (D) was 6–8 nm separated by an amorphous phase of ~ 1 nm. A power law relationship between the coercivity and grain size was observed with coercivity exhibiting a near D^3 dependency. These results are consistent with the nanostructure being dominated by long range uniaxial anisotropy.

¹M. A. Willard, J. C. Claassen, R. M. Stroud, T. L. Francavilla, and V. G. Harris, IEEE Trans. Magn. **38**, 3045 (2002).

²Y. Yoshizawa, S. Oguma, and K. Yamauchi, J. Appl. Phys. **64**, 6044 (1998).

³S. D. Joshi, S. D. Yoon, A. Yang, C. Vittoria, M. Willard, R. Goswami, and V. G. Harris, J. Appl. Phys. **99**, 08F115 (2006).

⁴J. D. Ayers, V. G. Harris, J. A. Sprague, W. T. Elam, and H. N. Jones, Acta Mater. **46**, 1861 (1998); J. D. Ayers, V. G. Harris, J. C. Sprague, W. T. Elam, and H. N. Jones, Nanostruct. Mater. **9**, 391 (1997); J. D. Ayers, V. G. Harris, J. C. Sprague, and W. T. Elam, Appl. Phys. Lett. **64**, 974 (1994).

⁵G. Herzer, IEEE Trans. Magn. **26**, 1397 (1990).

⁶K. Suzuki, G. Herzer, and J. M. Cadogan, J. Magn. Mater. **177–181**, 949 (1998).

⁷T. Swanson *et al.*, Natl. Bur. Stand. (U.S.) Circ. No. 539 (1955), Vol. IV, p. 3.

⁸T. Swanson *et al.*, Natl. Bur. Stand. (U.S.) Circ. No. 539 (1953), Vol. I, p. 13.

⁹C. J. Gutierrez, V. G. Harris, J. J. Krebs, W. T. Elam, and G. A. Prinz, J. Appl. Phys. **73**, 6763 (1993).